Equalisation of precession rates of galactic orbits (Part 2)

S. Edgeworth

11 May 2013

Abstract

A complete galactic component of uniform retrograde precession rate is constructed in the $\mathbf{f \propto d^2}$ field. The component has inner and outer boundaries, and is scale-free, so there may be multiple instances of the component, at various scales, nested within each other, each instance of the component having a different pattern speed.

A system of coplanar nested orbits is examined in a theoretical disk galaxy. Each of these orbits is assumed to be populated by a large number of stars.

In this second part of the investigation, we examine the theoretical galactic gravity field defined by $\mathbf{f \propto d^2}$. The force attracting a unit mass towards the galactic centre is proportional to the **square** of its distance from the galactic centre. Galactic orbits in this field are precessing ellipses centred on the galactic centre. The apsidal precession is in the retrograde direction (the opposite direction to the orbits). The precession rate of each orbit is a function of its axis ratio and its semi-major axis..

The system of units used is chosen so that a circular orbit of radius r=1, around a point mass m=1, has orbital velocity $v_{circ}=1$, angular velocity $\omega_{circ}=1$, and orbital period $T_{circ}=2\pi$. The axis ratio of an orbit is defined here as the minor axis divided by the major axis. The ellipticity is defined as 1 minus the axis ratio.

A C++ orbit integration computer program was adapted to work with any chosen centrally attractive axisymmetric force law. Additionally the program was given the ability to automatically detect when a star is at apocentre, and to measure the apsidal precession rate of each orbit. Initially a system of nested orbits is illustrated in figure 1, which have semi-major axes ranging from 0.10 to 1.05, and all have the same axis ratio = 0.4.

Figure 1: Nested orbits all with same axis ratio

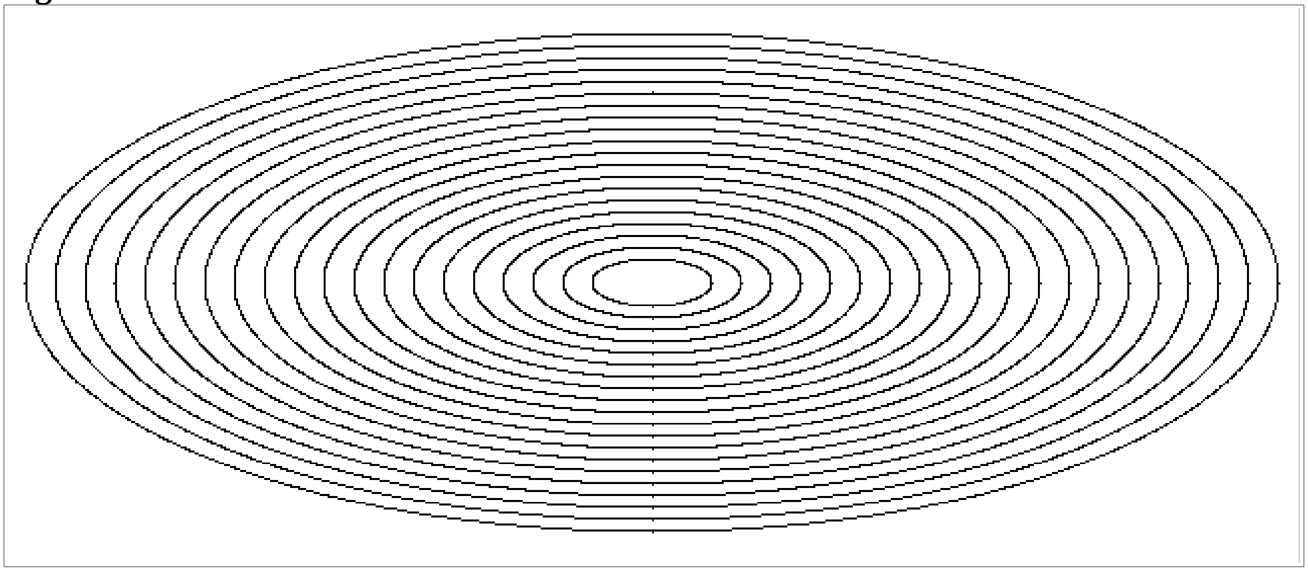

The precession rates of each of the orbits illustrated in figure 1 are calculated in the $\mathbf{f \propto d^2}$ field and listed in figure 2.

Figure 2: Unequalised precession rates in the $\mathbf{f \propto d^2}$ field

semi-major axis **a**	axis ratio **b/a**	precession rate $\boldsymbol{\omega_{prec}}$
0.10	0.4	-0.0024
0.15	0.4	-0.0045
0.20	0.4	-0.0069
0.25	0.4	-0.0096
0.30	0.4	-0.0126
0.35	0.4	-0.0159
0.40	0.4	-0.0194
0.45	0.4	-0.0232
0.50	0.4	-0.0272
0.55	0.4	-0.0313
0.60	0.4	-0.0357
0.65	0.4	-0.0402
0.70	0.4	-0.0450
0.75	0.4	-0.0499
0.80	0.4	-0.0550
0.85	0.4	-0.0602
0.90	0.4	-0.0656
0.95	0.4	-0.0711
1.00	0.4	-0.0768
1.05	0.4	-0.0826

If we examine any pair of adjacent orbits in figure 2, we find that both orbits precess in the retrograde direction, however the larger orbit precesses faster than the inner orbit. The different precession rates will cause the orbits to soon become intersecting and colliding, unless an interaction between each pair of adjacent orbits equalises their precession rates.

Here it is assumed that each pair of adjacent orbits interacts specifically by altering their orbital ellipticities, so as to equalise their precession rates, so that only tiny balancing torques are required to maintain a set of nested orbits in a state of equal precession. This results in a stable galactic component within which every orbit has a different ellipticity, and all orbits have the same precession rate.

A similar method has been applied by others (1) to provide one of the several possible explanations for precession-equalisation of orbits within an eccentric planetary ring.

The software does not directly model the orbital interactions. Instead the software is used to calculate the set of orbits which will result from the assumed ellipticity-modifying interactions.

In figure 3, a set of nested orbits is constructed in the $\mathbf{f \propto d^2}$ gravity field, with the ellipticity of each orbit carefully adjusted by software iteration, so that each orbit has the same precession rate.

Figure 3: Equalised precession rates in the $\mathbf{f \propto d^2}$ gravity field

semi-major axis **a**	axis ratio **b/a**	precession rate $\boldsymbol{\omega_{prec}}$
0.2	0.600	≈ -0.043
0.3	0.418	≈ -0.043
0.4	0.338	≈ -0.043
0.5	0.292	≈ -0.043
0.6	0.259	≈ -0.043
0.7	0.237	≈ -0.043
0.8	0.218	≈ -0.043
0.9	0.203	≈ -0.043
1.0	0.191	≈ -0.043
1.1	0.181	≈ -0.043
1.2	0.172	≈ -0.043

When one attempts to add new orbits, with semi-major axes significantly smaller than 0.2, or significantly larger than 1.2, it becomes impossible to match the precession rates of the new orbits to the uniform precession rate of the existing orbits. Therefore the component has an inner limit and an outer limit, beyond which the component cannot be expanded.

These orbits are illustrated in figure 4. The orbits are in the clockwise direction. The apsidal precession of each orbit is in the anti-clockwise direction (retrograde). All the orbits have the same precession rate.

Figure 4: Orbits with equalised precession rates in the $\mathbf{f \propto d^2}$ gravity field, with major axes aligned.

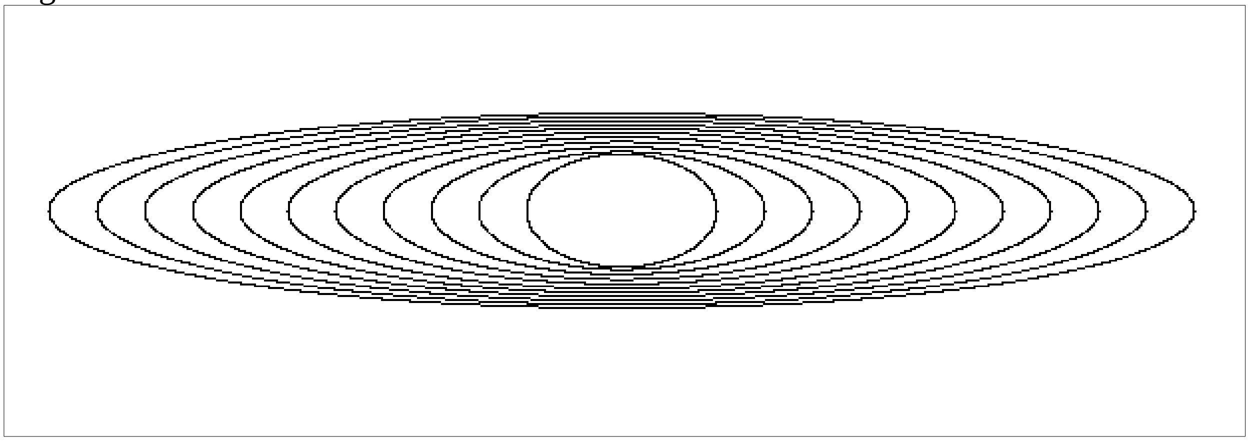

The same orbits are shown in figure 5, with major axes slightly differentially rotated, as they might be in their interactive state. The orbital direction is clockwise. All these orbits have the same retrograde precession rate. Note that the kinematic density waves are trailing.

Figure 5: Orbits with equalised precession rates in the $\mathbf{f \propto d^2}$ gravity field, with major axes differentially rotated.

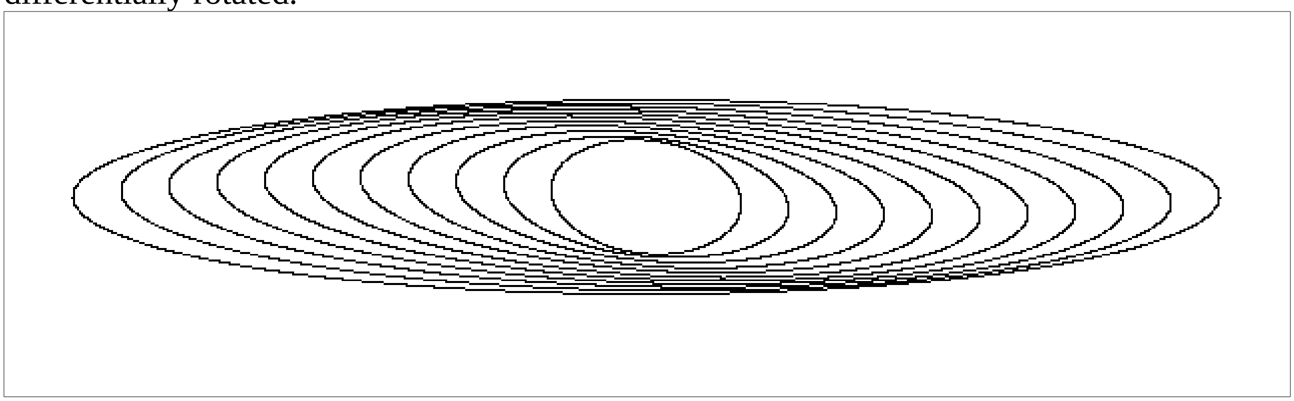

So the $\mathbf{f \propto d^2}$ field produces a component consisting of a set of nested orbits with a positive ellipticity gradient (orbit ellipticity increases with increasing orbit size), and with inner and outer limits..

The $\mathbf{f \propto d^2}$ field is scale-free, therefore the system of nested orbits illustrated in figures 4 and 5 can be constructed at any scale, by simply multiplying every semi-major axis value in figure 3 by a scaling constant **k**, and using the axis ratios of figure 3 unchanged. The result will be a new set of orbits, of exactly the same form and ellipticity profile, but at a different scale. All orbits in the new component will have a common precession rate ≈ $(-0.043 * \sqrt{\mathbf{k}})$.

Next we consider, in the $\mathbf{f \propto d^2}$ field, a galaxy in which the component illustrated in figures 4 and 5 already exists, but in which there are also many stars in a set of highly populated nested elliptic orbits beyond the outer limit of the existing component. The component has already been extended to its maximum outer limit. Synchronisation of the precession rates of these larger orbits with the precession rate of the existing component is not possible. So what structure will evolve in the outer, larger system of nested orbits?

To answer that question, first we draw an imaginary circle which exactly encloses the existing component, and note that a set of orbits, which is always outside that circle, will have no collisions with the existing component, and may therefore have a precession rate which differs from that of the the existing component. So, in the outer set of orbits, the interactions between each adjacent pair of orbits may adjust the ellipticity of the orbits, until their precession rates are equalised to a new precession rate.

So a new component may be constructed which encloses the existing component. On the assumption that the $\mathbf{f \propto d^2}$ field extends throughout the radial extents of both components, the new outer component has the same form and ellipticity profile as the existing inner component, but is scaled to a larger size.

Figure 6 illustrates the new larger set of nested orbits fitting neatly outside the existing component of figure 5, using a scaling constant **k**=10. The two components have identical ellipticity profiles. The inner component has retrograde pattern speed ≈ -0.043. The outer component has a faster retrograde pattern speed ≈ (-0.043 * √**k**) ≈ -0.136.

Figure 6: Two nested self-similar galactic components with different pattern speeds in the **$f \propto d^2$** gravity field

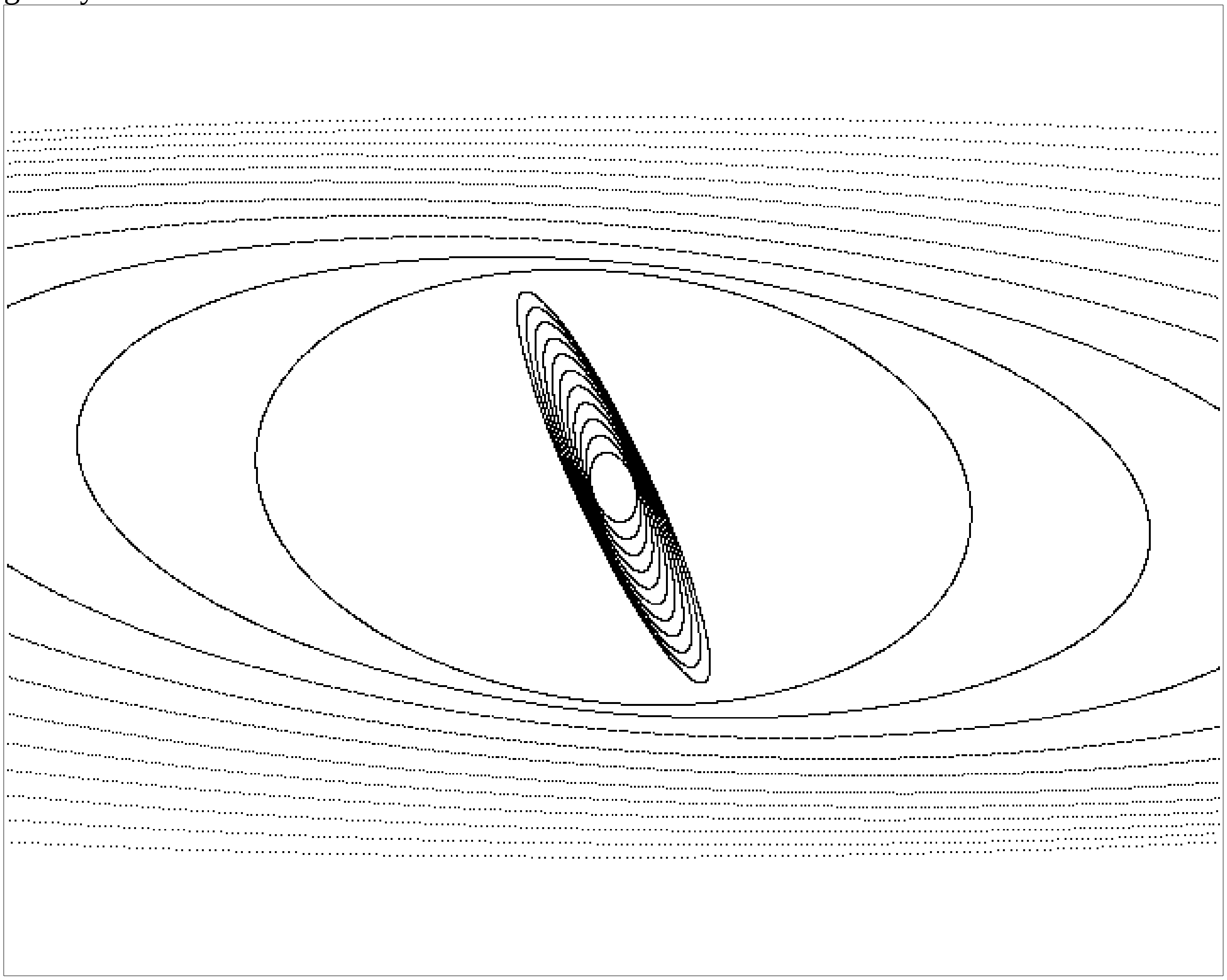

It is possible to continue the nesting further, so that three or more scaled instances of the component are nested.

In this paper, it is shown that the theoretical **$f \propto d^2$** field produces a galactic component with positive ellipticity gradient and retrograde pattern speed.

In the previous paper (4) it was shown that the theoretical **$f \propto \sqrt{d}$** field produces a galactic component with negative ellipticity gradient and prograde pattern speed.

Observation of real galaxies indicates that, where the direction of spiral arms can be determined unambiguously, they are usually trailing (2). In was demonstrated in the theoretical examination of the two fields above that, although the two fields have very different properties, both fields produce kinematic density waves which are usually trailing.

It is intended in the next paper (5) to generalise, where appropriate, the results obtained for those two fields, to two groups of power-law fields, either side of the harmonic $\mathbf{f \propto d}$ field (3), and also to refer to isophotal studies by others which illustrate real galactic components with positive ellipticity gradient, and with negative ellipticity gradient, respectively.

An online HTML5 simulation of a single galactic component comprising a set of orbits similar to those described above is available (6). The simulator has an option to select a co-rotating viewing frame, which rotates at the precession rate, making the co-precession of the orbits clear to see. It is the carefully tuned ellipticity gradient which produces the co-precession; without it the orbits would all have different precession rates. This paper has examined the $\mathbf{f \propto d^2}$ field. Please note that the online simulation is in the $\mathbf{f \propto d^{1.5}}$ field. However the galactic structure produced by co-precession is similar, in both of those fields.

References

(1) Murray, C., & Dermott, S.,
Solar System Dynamics,
(section 10.5.4, Eccentric and Inclined Rings).

(2) Binney, J. & Tremaine, S.,
Galactic Dynamics,
(section 6.1.1.d).

(3) Blitzer, L.,
Hyper-Elliptic Orbits,
1988CeMec..42..215B

(4) Equalisation of precession rates of galactic orbits (Part 1),
www.orbsi.uk/space/research/se/pdf/equalisation-precession-galactic-orbits-1.pdf

(5) Equalisation of precession rates of galactic orbits (Part 3),
www.orbsi.uk/space/research/se/pdf/equalisation-precession-galactic-orbits-3.pdf

(6) HTML5 simulation of a similar set of co-precessing orbits,
www.orbsi.uk/simulator/simulator.php?s=00032

---

v.5 30 Nov 2017 (removed java simulation, added HTML5 simulation).